J|A|C|S
COMMUNICATIONS

Published on Web 06/08/2006

Atomic-Scale Deformation in N-Doped Carbon Nanotubes

Chia-Liang Sun,[†] Houng-Wei Wang,[‡] Michitoshi Hayashi,*[,‡] Li-Chyong Chen,[‡] and Kuei-Hsien Chen*[,†]

Institute of Atomic and Molecular Sciences, Academia Sinica, Taipei 10617, Taiwan, and Center for Condensed Matter Sciences, National Taiwan University, Taipei 10617, Taiwan

Received December 28, 2005; E-mail: atmyh@ntu.edu.tw; chenkh@pub.iams.sinica.edu.tw

Point defects such as vacancies and interstitial atoms in bulk graphite have been studied since the early 1960s, and of late, it has been observed in carbon nanostructures.[1] The combination of hexagons and nonhexagonal rings can be responsible for curved carbon nanostructures.[2] For example, in one-dimensional (1D) carbon nanomaterials, the pentagon and heptagon are correlated to the positive and negative curvatures in the original straight 1D nanostructures.[2c] Besides those intrinsic defects, the studies on extrinsically doped carbon nanotubes (CNTs) have also been reported.[3] Among all the doped CNTs, the N-doped CNTs are of special interest in both fundamental and application studies.[4] The compartmentalized bamboo-like structure of N-doped CNTs has been attributed to the effect of N incorporation. Although there are many reports on N-doped CNTs, the basic understanding of the correlation between N dopants and the unique bamboo-like structure at the atomic level is still lacking.[5] The present study deals with the above aspect and is part of a continuing study in our laboratory to understand the catalytic activity related to N-doped CNTs for fuel cell applications. In this paper, the experimental observation of N incorporation in multiwalled carbon nanotubes (MWCNTs) is reported and correlated with the quantum chemistry calculation results on the atomic scale.[6] The results obtained from our calculation indicate that each arrangement of N atoms in CNTs produces their own local strains and results in their respective deformations.

Three typical kinds of N-bonding configurations are identified in doped CNTs, and other than molecular N_2, they can be classified as substitutional and pyridine-like dopant structures.[7] Figure 1 shows a series of transmission electron microscopy (TEM) images derived from the arrayed N-doped CNTs grown on Si substrates by microwave plasma-enhanced chemical vapor deposition.[4d] The TEM image of the so-called bamboo-like N-doped CNTs presented in Figure 1a clearly shows periodic interlinked structures inside the nanotubes. An energy-filtered N-mapping TEM image reveals that N is incorporated in the bamboo-like CNTs with nonuniform distribution (Figure 1c). It is observed that the interlinked parts in CNTs are brighter than the sidewall, which indicates increased N content in the former. Besides the above observation, which concurs with the previous report,[7a] further studies are needed in this direction to know more about the effect of N incorporation with bonding configurations on the tube surface. The understanding of different N-bonding configurations in CNTs will be useful, particularly in the field of catalysis and sensor technology.

We constructed finite cluster models of CNTs with pure and two different doping types to study the detailed structural changes at an atomic level. Geometry optimizations were preformed at the B3LYP/6-31G* density functional theory (DFT) level using Gaussian 03.[8] Figure 2 shows the optimized geometries and corresponding charge distribution plots of various cluster models for (a) undoped, (b) substitutional N-doped (sN-doped), and (c) pyridine-like N-doped (PyN-doped) zigzag (9,0) CNTs. Hydrogen termination at the ends of CNTs is introduced to avoid dangling bonds. For the last two doping cases, the doping concentrations were kept nominally at the same level of approximately 7 at. %, while six C

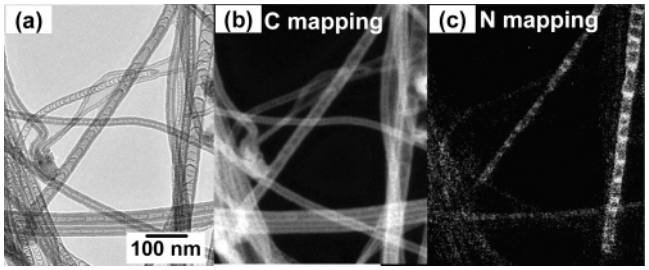

Figure 1. (a) TEM image of N-doped CNTs. Corresponding energy-filtered TEM (b) carbon and (c) nitrogen mapping images of N-doped CNTs.

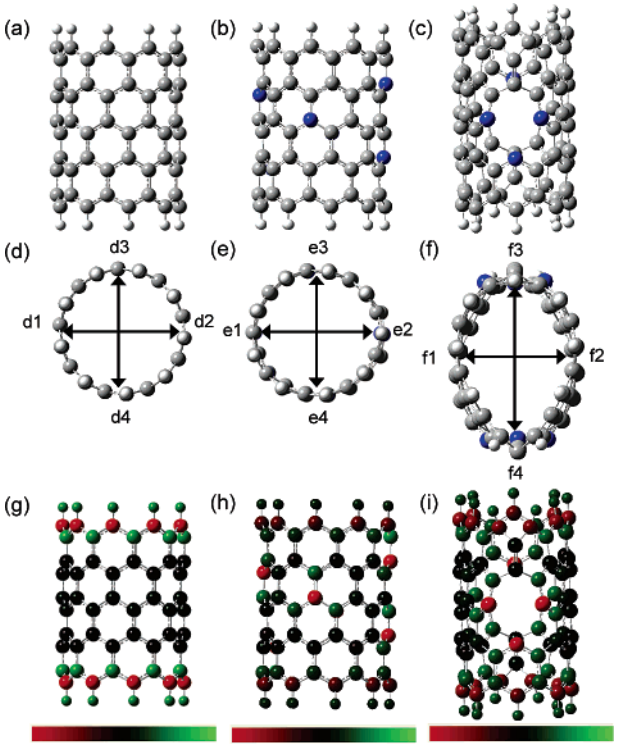

Figure 2. Optimized geometries of cluster models for (a) undoped ($C_{90}H_{18}$), (b) sN-doped ($C_{84}N_6H_{18}$), and (c) PyN-doped ($C_{82}N_6H_{18}$) zigzag (9,0) CNTs. C, N, and H atoms are gray, blue, and white spheres, respectively. (d−f) Corresponding cross-sectional views of these three (9,0) nanotube clusters. (g−i) Corresponding charge distribution plots of the three clusters. The color bars are related to the charge values from the most negative (red, left) one gradually to the most positive (green, right) one.

[†] Academia Sinica.
[‡] National Taiwan University.

10.1021/ja0587852 CCC: $33.50

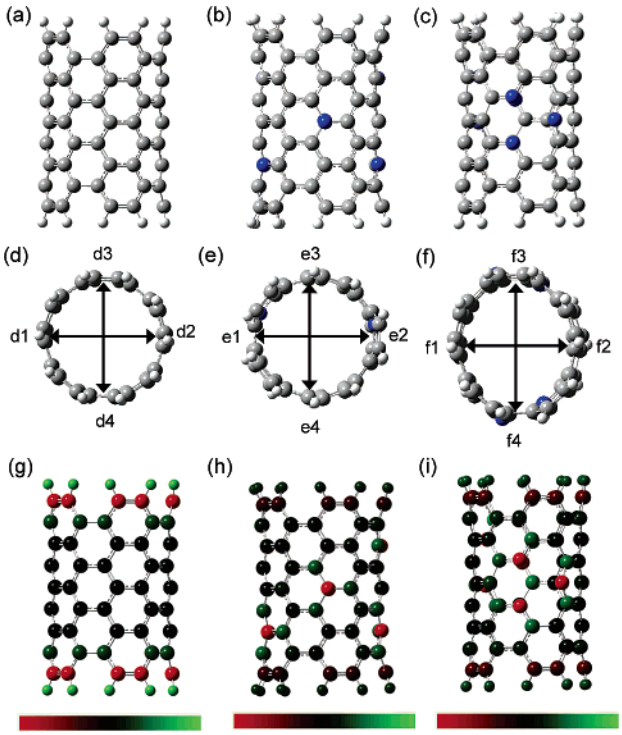

Figure 3. Optimized geometries of cluster models for (a) undoped ($C_{90}H_{20}$), (b) sN-doped ($C_{84}N_6H_{20}$), and (c) PyN-doped ($C_{82}N_6H_{20}$) armchair (5,5) CNTs. C, N, and H atoms are gray, blue, and white spheres, respectively. (d−f) Corresponding cross-sectional views of these three (5,5) nanotube clusters. (g−i) Corresponding charge distribution plots of the three clusters. The color bars are related to the charge values from the most negative (red, left) one to the most positive (green, right) one.

atoms were replaced by N atoms. Moreover, it is noteworthy that we have adopted the pyridine-like structure proposed in the literature.[4c] In this structure, we removed a central C atom to create a vacancy among three hexagons, and then three C atoms around it were replaced by N atoms. By doing so, as seen in Figure 1, the PyN-doped CNT is distorted drastically, and it is very clear when we visualize it through the cross sections. The two perpendicular distances across the cross sections are used to describe the deformed structures. As shown in Figure 2d−f, the ratio of these two perpendicular distances is close to ∼1 in the undoped and sN-doped cases. Both of them have circular cross sections along the diameter, and in the sN-doped case, it was slightly enlarged. In contrast, as shown in Figure 3d−f, the ratio is significantly changed to 0.71, resulting in an ellipsoid-like cross section when N atoms are closely arranged to form the pyridine-like structure. This kind of local distortion induces a positive curvature in the graphene layer. This implies that the concentrated N atoms are responsible for the tube wall roughness, and the bamboo structures are due to terminated inner layers with higher N concentrations in MWCNTs. Figure 2g−i illustrate the corresponding charge density plots of these three clusters. They show that the N atoms with lone pair electrons always bring the very negative charges and are marked in red color. More details on the structural deformation and the charge values can be found in the Supporting Information.

Figure 3 shows the optimized geometries of cluster models for (a) undoped, (b) sN-doped, and (c) PyN-doped armchair (5,5) CNTs. Their cross sections and charge density plots are also shown in Figure 3d−f and Figure 3g−i, respectively. Interestingly, they exhibit similar behavior as that of zigzag cases, except that the extent of distortion is less. The cross-section analysis of the PyN-doped (5,5) cluster shows that the axis along the pyridine sites is not elongated very much and the distance ratio reaches only up to 0.94. However, the charge distribution values are very similar to the armchair (9,0) clusters, and the cross-sectional area is also enlarged. This discrepancy in the results found among zigzag and armchair cases could be attributed to the limited orientations of their PyN sites. The calculation results indicate that the two-third N atoms and the hexagons in the PyN site of armchair CNTs must be in parallel with the tube axis. This kind of orientation sustains less bending stress in comparison with those aligned with the radial direction in zigzag CNTs.

In conclusion, the N-doping induced atomic-scale structural deformation in CNTs has been investigated by using DFT calculations. The homogeneously distributed, isolated N dopants in sN-doped clusters enlarge the tube diameter. In other words, the deformed structures observed in the experiment can be ascribed to the concentrated N dopants in PyN sites.

Acknowledgment. We gratefully acknowledge the financial support by National Science Council (NSC) and the National Center for High-performance Computing in Taiwan.

Supporting Information Available: The full list of authors in ref 8, dimensional changes in a variety of cluster models for CNTs, and information about the double-walled CNT, capped CNT, and molecular orbitals. This material is available free of charge via the Internet at http://pubs.acs.org.

References

(1) (a) Backer, C.; Kelly, A. *Nature* **1962**, *193*, 236−236. (b) Kelly, B. T. *Nature* **1965**, *207*, 257−259. (d) Ajayan, P. M.; Ravikumar, V.; Charlier, J. C. *Phys. Rev. Lett* **1998**, 1437−1440. (e) Hashimoto, A.; Suenaga, K.; Gloter, A.; Urita, K.; Iijima, S. *Nature* **2004**, *430*, 870−873.

(2) (a) Kroto, H. W.; Heath, J. R.; O'Brien, S. C.; Curl, R. F.; Smalley, R. E. *Nature* **1985**, *318*, 162−163. (b) Kroto, H. W. *Nature* **1987**, *329*, 529−531. (c) Iijima, S.; Ichihashi, T.; Ando, Y. *Nature* **1992**, *356*, 776−778. (d) Murry, R. L.; Strout, D. L.; Odom, G. K.; Scuseric, G. E. *Nature* **1993**, *366*, 162−163. (e) Krishnan, A.; Dujardin, E.; Treacy, M. M. J.; Hugdahl, J.; Lynum, S.; Ebbesen, T. W. *Nature* **1997**, *388*, 451−454.

(3) (a) Zhou, O.; Fleming, R. M.; Murphy, D. W.; Chen, C. H.; Haddon, R. C.; Ramirez, A. P.; Glarum, S. H. *Science* **1994**, *263*, 1744−1747. (b) Stephan, O.; Ajayan, P. M.; Colliex, C.; Redlich, Ph.; Lambert, J. M.; Bernier, P.; Lefin, P. *Science* **1994**, *266*, 1683−1685. (c) Lee, R. S.; Lim, H. J.; Fischer, J. E.; Thess, A.; Smalley, R. E. *Nature* **1997**, *388*, 255−257. (d) Rao, A. M.; Ekland, P. C.; Bandow, S.; Thess, A.; Smalley, R. E. *Nature* **1997**, *388*, 257−259. (e) Endo, M.; Muramutsu, H.; Hayashi, T.; Kim, Y. A.; Lier, G. V.; Charlier, J. C.; Terrones, H.; Terrones, M.; Dresselhaus, M. S. *Nano Lett.* **2005**, *5*, 1099−1105.

(4) (a) Terrones, M.; Grobert, N.; Olivares, J.; Zhang, J. P.; Terrones, H.; Kordatos, K.; Hsu, W. K.; Hare, J. P.; Townsend, P. D.; Prassides, K.; Cheetham, A. K.; Kroto, H. W.; Walton, D. R. M. *Nature* **1997**, *388*, 52−55. (b) Sen, R.; Satishkumar, B. C.; Govindaraj, A.; Hairkumar, K. R.; Renganathan, M. K.; Rao, C. N. R. *J. Mater. Chem.* **1997**, *7*, 2335−2337. (c) Czerw, R.; Terrones, M.; Charlier, J. C.; Foley, B.; Kamalakaran, R.; Grobert, N.; Terrones, H.; Tekleab, D.; Ajayan, P. M.; Blau, W.; Rühle, M.; Carroll, D. L. *Nano Lett.* **2001**, *1*, 457−460. (d) Chen, L. C.; Wen, C. Y.; Liang, C. H.; Hong, W. K.; Chen, K. J.; Cheng, H. C.; Shen, C.S.; Wu, C. T.; Chen, K. H. *Adv. Funct. Mater.* **2002**, *12*, 687−692. (e) Sun, C. L.; Chen, L. C.; Su, M. C.; Hong, L.S.; Chyan, O.; Hsu, C. Y.; Chen, K. H.; Chang, T. F.; Chang, L. *Chem. Mater.* **2005**, *17*, 3749−3753.

(5) Klein, B. M. *Nature* **1999**, *399*, 108−109.

(6) (a) Lu, X.; Chen, Z.; Schleyer, P. v. R. *J. Am. Chem. Soc.* **2004**, *127*, 20−21. (b) Piva, P. G.; DiLabio, G. A.; Pitters, J. L.; Zikovsky, J.; Rezeq, M.; Dogel, S.; Hofer, W. A.; Wolkow, R. A. *Nature* **2005**, *435*, 658−661. (c) Nikawa, H.; Kikuchi T.; Wakahara, T.; Nakahodo, T.; Tsuchiya, T.; Rahman, G. M. A.; Akasaka, T.; Maeda, Y.; Yoza, K.; Horn, E.; Yamamoto, K.; Mizoroji, N.; Nagase, S. *J. Am. Chem. Soc.* **2005**, *127*, 9684−9685.

(7) (a) Han, W. Q.; Kohler-Redlich P.; Seeger, T.; Ernst, F.; Grobert, N.; Hsu, W. K.; Chang, B. H.; Zhu, Y. Q.; Kroto, H. W.; Walton, D. R. M.; Terrones, M.; Terrones, H. *Appl. Phys. Lett.* **2000**, *77*, 1807−1809. (b) Reyes-Reyes, M.; Grobert, N.; Kamalakaran, R.; Seeger, T.; Golberg, D.; Rühle, M.; Bando, Y.; Terrones, H.; Terrones, M. *Chem. Phys. Lett.* **2004**, *396*, 167−173. (c) Choi, H. C.; Bae, S. Y.; Park, J.; Seo, K.; Kim, C.; Kim, B.; Song, H. J.; Shin, H. J. *Appl. Phys. Lett.* **2004**, *85*, 5742−5744.

(8) Frisch, M. J. et al. *GAUSSIAN 03*; Gaussian, Inc.: Wallingford, CT, 2004.

JA0587852